

Experimental comparison of all-optical methods of chromatic dispersion compensation in long haul transmission at speeds of 10 Gbit/s

J. Vojtěch,^{1,*} M. Karásek,^{1,2} and J. Radil¹

¹CESNET a.l.e., Zikova 4, 160 00 Prague 6, Czech Republic

²Institute of Photonics and Electronics, Academy of Sciences of the Czech Republic, Chaberská 77, Czech Republic

*Corresponding author: josef.vojtech@cesnet.cz

Received July 23, 2007; revised September 20, 2007;
accepted October 19, 2007; published November 14, 2007 (Doc. ID 85536)

Different techniques and scenarios of all-optical chromatic are compared experimentally. Chromatic dispersion was compensated both conventionally by dispersion compensating fibers and unconventionally using both channelized and broadband fiber Bragg gratings and Gires–Tournois etalons. Results are compared experimentally at a transmission speed of 10 Gbit/s. Emphasis was also given to tunability and broadband characteristics of elements. © 2007 Optical Society of America

OCIS codes: 060.2330, 060.4230, 260.2030.

1. Introduction

Standard single-mode fibers [(SSMFs) ITU-T specification: G.652] represent the majority of already installed fibers. SSMFs were designed for operation in O-band and thus their wavelength of zero chromatic dispersion (CD) is close to 1310 nm. Their low loss in C-band and the availability of reliable and relatively cheap erbium-doped fiber amplifiers (EDFAs) make the 1550 nm window attractive for multichannel high-speed transmission. Unfortunately within this window SSMF exhibits relatively large CD, approximately +16.8 ps/(nm*km), which severely limits transmission distance at transmission rates of 10 Gbit/s and higher unless compensated. Although this issue has been alleviated by introducing nonzero dispersion shifted fibers (NZ DSFs), these fibers represent a minority of the installed fiber base and their usage under high channels counts (resulting in higher power density due to smaller effective area compared to SSMF) is considered problematic. Today, the effect of CD can be mitigated by various methods. These range from application of all-optical components to electronics-based subsystems. As electrical processing is generally performed on a per channel basis, all-optical CD compensation methods are superior for systems based on wavelength division multiplexing (WDM). Therefore we will focus on all-optical techniques.

Most frequently, dispersion compensating fibers (DCFs) that exhibit negative CD typically in the range from $D = -95$ to -250 ps/(nm*km) [1] are used. Unfortunately, they also have a higher insertion loss (IL) compared with transmission fibers. Currently DCFs with IL ranging from 0.43 to 0.64 dB/km are commercially available. Although DCF is a broadband element, the dispersion slopes of SSMF and DCF are not exactly balanced. For WDM systems, the wavelength dependence of residual dispersion is usually required to be within the limits of the system dispersion tolerance.

A less often used element for CD compensation is a chirped fiber Bragg grating (FBG) [2–4]. At the beginning, channelized FBGs were designed to compensate CD of the 100 GHz or 50 GHz spaced channels—typically at the wavelengths' grid defined by Telecommunication Standardization Sector of the International Telecommunications Union (ITU-T). Currently available FBGs are, however, broadband, covering even an entire telecom band. Main advantages of CD compensators based on FBG are low IL and the possibility of designing compensation modules to exactly match the

Table 1. Compensators Compensating CD of 100 km SSMF—Insertion Losses

| CD Compensators | IL [dB] |
|------------------------------|---------|
| DCF 13.8 km | 6.2 |
| Broadband FBG | 3.5 |
| Channelized FBG ^a | 2.9 |
| GTE ^a | 2 |
| PA ^a | 8 |

^aA tunable version is also available for this compensator

dispersion slope of the transmission fiber. The disadvantage of fixed FBG modules is that they must be tailored to compensate certain transmission fiber length, similar to DCF modules.

Tunability of CD compensation becomes crucial with increasing transmission bit rate because the tolerance of receivers to accumulated CD decreases with the square of transmission rate. For example, existing 40 Gbit/s non-return-to-zero (NRZ) receivers can tolerate residual CD of approximately 100 ps/nm only. Furthermore, in reconfigurable networks, accumulated CD can change due to the rerouting of the optical path and thus variable CD compensation is required. There are several possibilities to achieve tunable CD compensation, including differential thermal tuning of nonlinearly chirped FBG [5,6], thermal tuning of free space or FBG coupled-cavities Gires-Tournois etalons (GTEs) [7,8], and virtually imaged phase arrays (PAs) [9,10]. Typical insertion loss of the most frequently used CD compensators is summarized in Table 1. As indicated by ^a, tunable versions are available for some compensators. Full CD compensation of 100 km of SSMF (approximately +1680 ps/nm) is assumed for the comparison.

Commercially available transmission systems usually rely on the traditional approach, where DCF modules are inserted periodically, typically after 80 km of SSMF. Relatively high losses of DCF are compensated using dual stage EDFA configuration. In an alternative approach DCF modules are optically pumped and used as a medium for Raman amplification, thus converting loss elements to elements with gain [1,11].

Design of research and educational networks (RENs) frequently differs from regular telecom networks. In many countries, RENs are based on leased dark fibers. Often it is not possible to deploy inline equipment (both amplifiers and CD compensators) or it is not economical. However “shorter” links, up to 250 or 300 km, can be lighted using the so-called “nothing inline” approach, where transmission equipment is deployed only in terminal nodes [12,13]. In the last ten years, many papers dealing with CD compensation and management in telecom transmission systems have been published, e.g., [14]. On the other hand, CD compensation management in nothing inline scenarios has not been addressed in detail yet, maybe due to the difficulties resulting from relatively high signal powers in transmission fibers.

In this paper, we present experimental results for the application of different CD compensation scenarios utilizing traditional DCFs, channelized FBGs, channelized tunable FBGs (TFBGs), broadband FBGs, and tunable GTEs. Eight 10 Gbit Ethernet (GE) channels were transmitted over 225 km of SSMF without application of inline EDFAs. Susceptibility of the transmission quality to residual chromatic dispersion and input signal power has been investigated. Transmission quality of one of the channels has been tested by the EXFO Packet Blazer 10 GE FTB-5810G module.

2. Experimental Setup

The referential laboratory setup based on DCF modules is shown in Fig. 1. Signals from eight dense wavelength division multiplex (DWDM) 10 Gbit small form factor pluggable (XFP) transceivers (Finisar FTLX3811M3) were combined in a multiplexer (MUX), amplified in a high-power C-band EDFA, and launched into the test fiber link. Wavelengths of the transmitted channels (TX₁–TX₄) were 1550.12–1552.52 nm, channels 34–31 according to ITU 100 GHz grid, wavelengths of transmitters TX₅–TX₈ were 1554.13–1556.56 nm, ITU channels 29–26. Transmitter output power was typically 1 mW, nominal receiver sensitivity was –24 dBm, and CD tolerance was claimed to be 1600 ps. The test link consisted of 225 km of SSMF on spools, with granularity 50 and

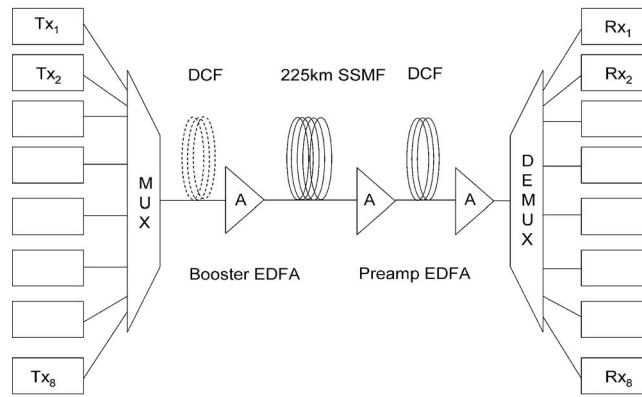


Fig. 1. DCF-based experimental setup.

25 km. The CD of the link was $\approx +3780$ ps/nm; the link loss was 49 dB. At the receiver side, signals were first amplified in a low noise EDFA, accumulated CD was compensated using one of the available compensating techniques, and finally demultiplexed in a demultiplexer (DEMUX). Transceiver 4 (1552.52 nm) was inserted in bit-error ratio (BER) tester Packet Blazer 10 GE FTB-5810G module. The BER tester was operated as a layer 2 tester in a loopback regime. We used the 2^{31} test pattern with the longest frame size of 1518 bytes and performed each measurement for 20 min. This represents $\approx 10^9$ of transmitted frames. The tester detects the number of properly received frames. The ratio of nonproperly (lost or badly) received to transmitted frames is evaluated as frame error.

In the first experiments, four DCF modules (OFS EWBDK), designed for compensating 1370, 946, 689, and 343 ps/nm were used. Optional CD precompensation has also been tested and is depicted as a dashed line DCF between MUX and booster EDFA in Fig. 1. It was necessary to use two EDFAs at the receiver side to eliminate the DCF attenuation. Total output power at the first preamp EDFA output (i.e., launched into DCF) was kept at 0 dBm. When DCFs were replaced by alternative compensating elements with a lower insertion loss it was possible to simplify the setup, as shown Fig. 2. In further experiments we used the following compensators: channelized FBGs (both fixed and tunable), fixed broadband FBGs, and tunable GTEs.

The fixed FBGs (TeraXion, ClearSpectrum) were designed for 100 GHz channel spacing. For target dispersion of -3500 ps/nm they typically exhibit polarization mode dispersion 1.5 ps, insertion loss <3.2 dB, and polarization dependent loss <0.05 dB. The temperature tunable FBGs (TeraXion, TDCM51) were designed for 100 GHz channel spacing and dispersion range from -1200 to -2700 ps/nm. They typically exhibit polarization mode dispersion 1.9 ps, insertion loss <4.7 dB, and polarization dependent loss <0.2 dB. We tested three broadband (unchannelized) FBG modules (Proximion DCM-DB) designed to compensate 80, 100, and 120 km of G.652 fiber (1344, 1680, 2016 ps/nm). Typical parameters are: wavelength range 1528–1570 nm, insertion loss <3 dB, polarization dependent loss <0.1 dB, and polar-

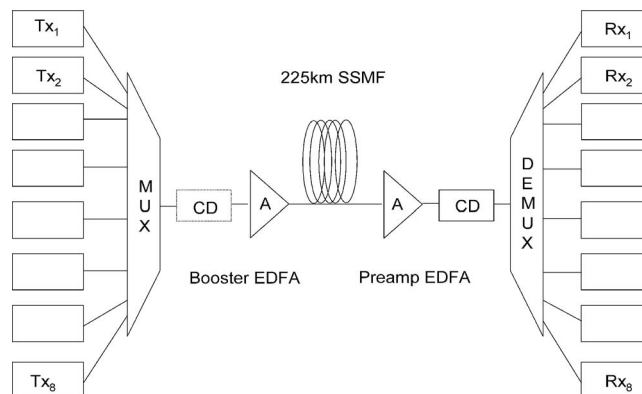


Fig. 2. Unconventional elements based experimental setup.

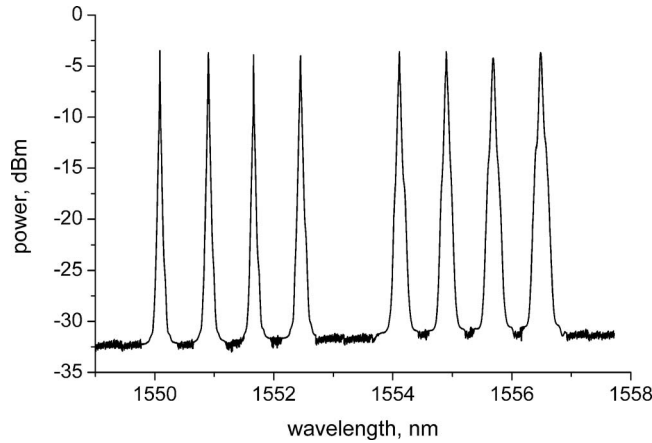


Fig. 3. Optical power at the output of the MUX.

ization mode dispersion <2.5 ps. The tunable GTEs (Civcom TODC) provide dispersion value ranging from -1700 to +1700 ps/nm and are based on four GTEs that cascade in free space. Typical parameters are: operating wavelength 1528–1564 nm, channel spacing 50 GHz, insertion loss <2 dB, polarization dependent loss <0.3 dB, and tuning resolution 100 ps/nm.

3. Results

Figure 3 shows the optical power at the output of the MUX. It can be seen that the power of individual transmitters is almost the same and at the MUX output equal to ≈ -3 dBm. In the reference experiments, CD was compensated using DCF modules. Figure 4 shows the frame error ratio as a function of total input power (denoted in the text as composite input power) launched into the transmission fiber, P_{in} , with the amount of compensated CD as a parameter to demonstrate the tolerance of transmission quality to signal power. The composite input power was taken from the monitoring power meter of the commercial EDFA booster. The postcompensation scheme depicted in Fig. 1 was used. It follows from Fig. 4 that the best performance was achieved when the dispersion compensation ratio (DCR) was 61%. In this case the lowest detectable frame error ratio of 10^{-9} was obtained for composite input signal power in the range of 24 to 29 dBm (i.e., 15 to 20 dBm/channel). The dispersion compensation ratio is defined as

$$DCR = \frac{|CD_{CDCM}|}{D_{TF}L_{TF}},$$

where D_{TF} in ps/nm/km and L_{TF} in km are the dispersion coefficients and the length of the transmission fiber, respectively. CD_{CDCM} is the chromatic dispersion of the dispersion compensating module in ps/nm. In the case of the DCF module it equals

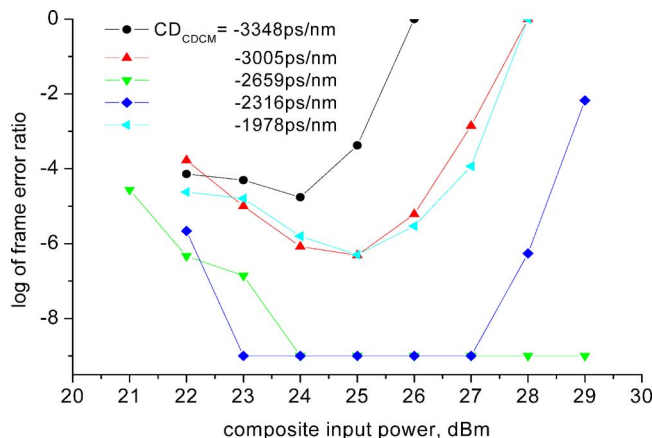


Fig. 4. Transmission tolerance to input power—DCF postcompensation.

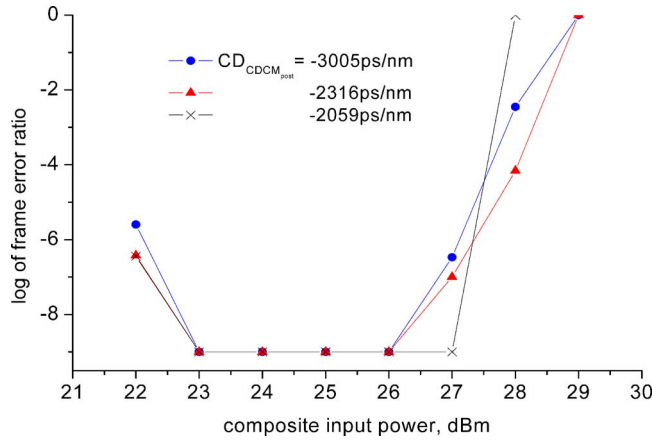


Fig. 5. Transmission tolerance to input power—DCF partial precompensation.

$D_{DCF} * L_{DCF}$. The worst performance was achieved when the DCR was $\approx 90\%$. Figure 5 shows the tolerance of transmission quality to total input power launched into the transmission fiber when CD was partially precompensated by 340 ps/nm. The amount of postcompensated CD is a parameter. The range of allowable input power is narrower compared to the pure postcompensation scheme, but the frame error ratio is less sensitive to total DCR. Frame error ratio better than 10^{-9} has been measured for per channel power in the range of 14 to 17 dBm for DCR=62%, 70%, and 88%.

In the next experiments, CD was compensated by one of the following all-optical methods: channelized FBGs, channelized tunable FBGs (TFBGs), broadband FBGs, and tunable GTEs.

Figure 6 demonstrates the tolerance to composite input power launched into the link for different compensating methods. The value of compensated CD was fixed at 3400 ps/nm, which represents residual dispersion of the link $\approx +380$ ps/nm (DCR =90%). The lowest frame error ratio of 10^{-9} has been reached for composite input power in the range of at least 2 dB, while with the DCF postcompensation scheme (Fig. 4) and the same residual dispersion the lowest frame error ratio has not been achieved. The best performance gives two concatenated GTEs.

Next, tolerance to input power for different values of compensated CD was examined using tunable elements (two cascaded channelized TFBGs or GTEs) and broadband FBGs (all three modules available were combined) in postcompensation configuration. Figures 7–9 plot the frame error ratio as a function of total signal input power for broadband FBGs, tunable channelized FBGs, and tunable GTEs, respectively. It is clear from Fig. 7 that the worst performance has occurred when two wideband FBG modules (1344 plus 2016 ps/nm) were used (residual dispersion $\approx +84$ ps/nm, DCR =98%). Application of tunable channelized FBG and GTE modules results in similar frame error ratio when 3200 and 3400 ps/nm of link CD were compensated.

Figures 10 and 11 compare recorded eye diagrams for tunable GTEs at receiver 4,

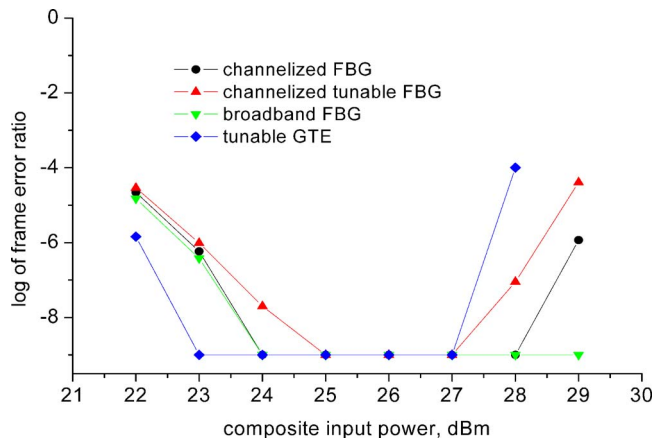


Fig. 6. Transmission tolerance to input power—unconventional elements postcompensation.

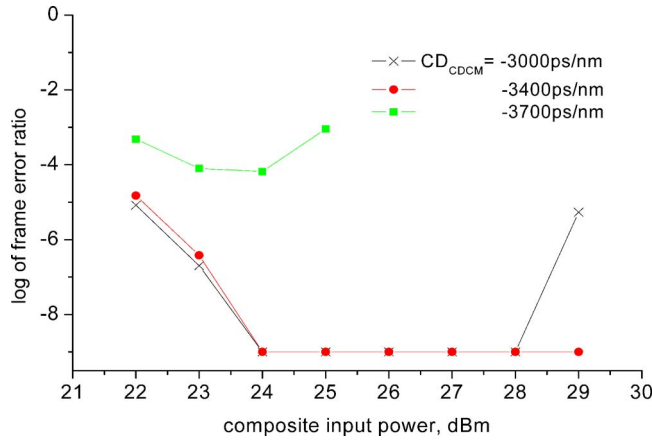


Fig. 7. Transmission tolerance to input power—broadband FBGs postcompensation.

$P_{in}=25$ dBm (16 dBm/channel). Figure 10 corresponds to DCR=80% ($CD_{CDCM}=3000$ ps/nm) and Fig. 11 to DCR=90% ($CD_{CDCM}=3400$ ps/nm). It can be seen that for DCR=80% (frame error ratio 10^{-5} , see Fig. 9) the eye diagram is deformed in marks and the eye opening is comparable with the case of DCR=90% (frame error ratio 10^{-9}). This is in agreement with our previous results [15]. Then we fixed the launched signal power to $P_{in}=25$ dBm and investigated the effect of DCR on transmission quality using tunable FBG or GTE modules. In Fig. 12 results for the partial precompensation scenario are summarized. As a precompensation module we used the -670 ps/nm DCF module; dispersion of the postcompensation module was varied in steps of 100 ps/nm. With GTEs we were limited by the aggregate maximum negative

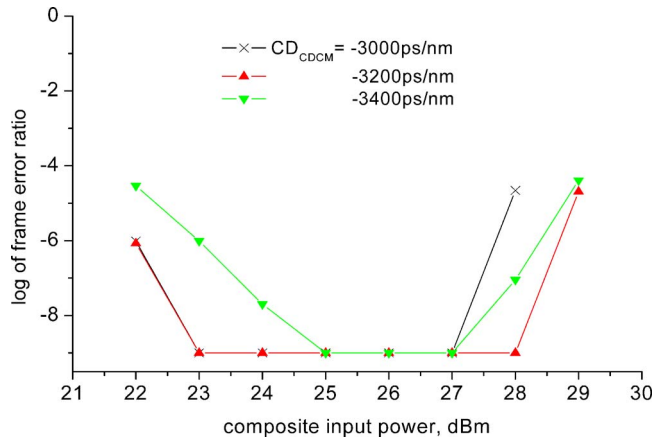


Fig. 8. Transmission tolerance to input power—channelized TFBGs postcompensation

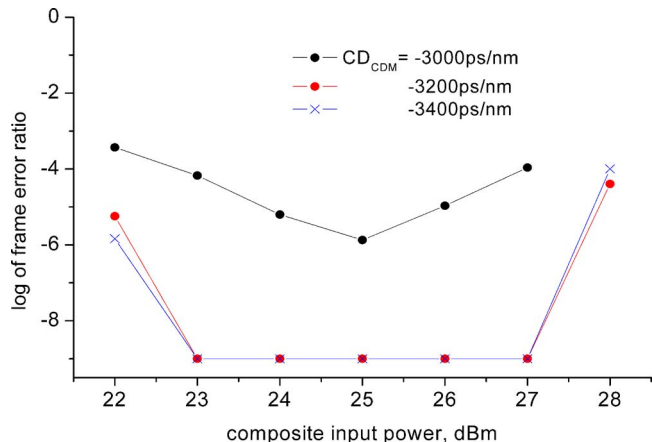


Fig. 9. Transmission tolerance to input power—tunable GTEs postcompensation.

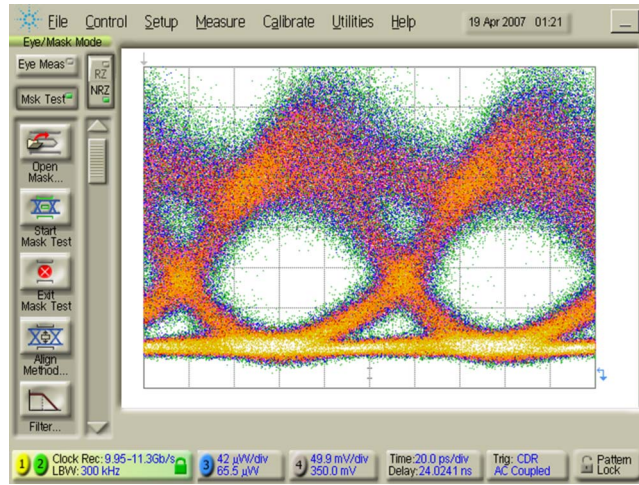


Fig. 10. Eye diagram at receiver 4, $P_{in}=25$ dBm, DCR=80%—tunable GTEs postcompensation.

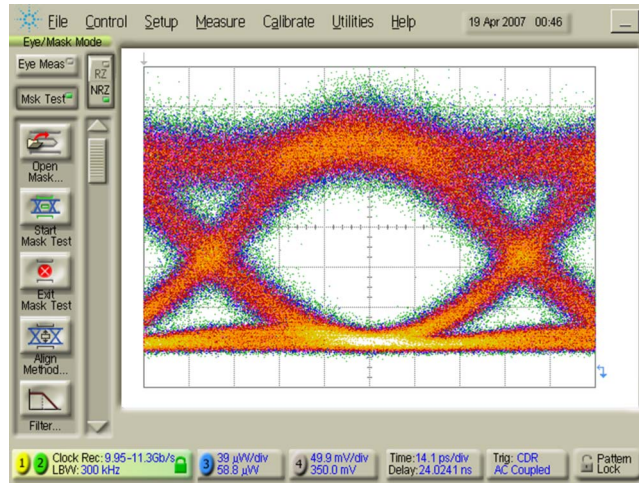


Fig. 11. Eye diagram at the receiver 4, $P_{in}=25$ dBm, DCR=90%—tunable GTEs postcompensation.

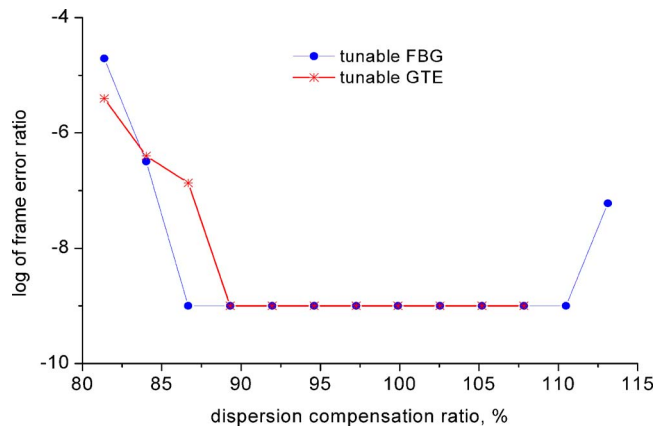


Fig. 12. Frame error ratio as a function of dispersion compensation ratio—partial pre-compensation with -670 ps/nm, $P_{in}=16$ dBm/channel.

dispersion of the two modules at -3400 ps/nm. It follows from Fig. 12 that application of tunable FBG modules allows for higher tolerance to residual dispersion compared with GTE modules, and even the overcompensated link ($\text{DCR} < 110\%$) resulted in frame error ratio $< 10^{-9}$.

4. Conclusion

We experimentally investigated different CD compensation techniques in nothing-in-line setups. We used traditional DCF modules, fixed channelized and broadband FBGs, tunable FBGs, and tunable GTE modules. Tests were performed by transmitting 8×10 GE channels over 225 km of SSMFs; signals were amplified at transmitter and receiver sides by standard C-band EDFAs. Experiments confirmed that unconventional elements enable implementation of simpler setups due to lower insertion loss compared with DCFs. Furthermore, we can conclude that for error-free transmission the GTEs allow launching of lower input powers, in contrast to broadband FBGs, which can tolerate higher launch powers and therefore longer span length. When comparing tunable devices we can state that FBGs enable error-free operation over broader ranges of input power and residual chromatic dispersion, compared with GTEs. However, GTEs offer tunable CD compensation with very low IL at reasonable prices. Experimental setups based on partial CD precompensation proved that small CD precompensation (≈ -340 ps/nm) can dramatically increase transmission CD tolerance. We believe this is due to suppression of self-phase modulation in the link.

By comparing eye diagrams of the error-free transmission and transmission with the frame error ratio $> 10^{-9}$ corresponding to the same per channel signal power well below the threshold for the occurrence of nonlinear effects, we can conclude that the transmission is mainly limited by improper compensation of chromatic dispersion of the link. This is in agreement with our previous results performed for single channel transmission without inline EDFAs.

In the future we would like to experimentally verify applicability of virtually imaged phase-array CD compensators, both fixed and tunable. The results of the performed experiments will be utilized in various projects related to the national optical research and educational network CESNET2 and experimental optical facility Czech-Light.

Acknowledgments

This research has been supported by the Ministry of Education, Youth, and Sport of the Czech Republic under research plan MSM6383917201, Optical National Research Network and Its New Applications, and project 1P05OC001.

References

1. L. Grüner-Nielsen, M. Wandel, P. Kristensen, C. Jørgensen, L. V. Jørgensen, B. Edvold, B. Pálsdóttir, and D. Jakobsen, "Dispersion-compensating fibers," *J. Lightwave Technol.* **23**, 3566–3577 (2005).
2. W. H. Loh, R. I. Laming, N. Robinson, A. Cavaciuti, F. Vaninetti, C. J. Anderson, M. N. Zervas, and M. J. Cole, "Dispersion compensation over distances in excess of 500 km for 10-Gb/s systems using chirped fiber gratings," *IEEE Photon. Technol. Lett.* **8**, 944–946 (1996).
3. Y. Painchaud, A. Mailloux, H. Chotard, É. Pelletier, and M. Guy, "Multi-channel fiber Bragg gratings for dispersion and slope compensation," in *Optical Fiber Communication Conference*, A. Sawchuk, ed., Vol. 70 of OSA Trends in Optics and Photonics (Optical Society of America, 2002), paper ThAA5.
4. Y. Painchaud, M. Poulin, M. Morin, and M. Guy, "Fiber Bragg grating based dispersion compensator slope-matched for LEAF fiber," in *Optical Fiber Communication Conference and Exposition and the National Fiber Optic Engineers Conference*, Technical Digest (CD) (Optical Society of America, 2006), paper OThE2.
5. Y. W. Song, D. Starodubov, Z. Pan, Y. Xie, A. E. Willner, and J. Feinberg, "Tunable WDM dispersion compensation with fixed bandwidth and fixed passband center wavelength using a uniform FBG," *IEEE Photon. Technol. Lett.* **14**, 1193–1195 (2003).
6. R. L. Lachance, S. Lelièvre, and Y. Painchaud, "50 and 100 GHz multichannel tunable chromatic dispersion slope compensator," in *Optical Fiber Communication Conference*, Technical Digest (Optical Society of America, 2003), paper TuD3.
7. B. J. Vakoc, W. V. Sorin, and B. Y. Kim, "A tunable dispersion compensator comprised of cascaded single-cavity etalons," *IEEE Photon. Technol. Lett.* **17**, 1043–1045 (2005).
8. S. Doucet, R. Slavik, and S. LaRochelle, "Tunable dispersion and dispersion slope

- compensator using novel Gires-Tournois Bragg grating coupled-cavities," *IEEE Photon. Technol. Lett.* **16**, 2529–2531 (2004).
9. M. Shirasaki and S. Cao, "Compensation of chromatic dispersion and dispersion slope using a virtually imaged phased array," in *Optical Fiber Communication Conference*, 2001 OSA Technical Digest Series (Optical Society of America, 2001), paper TuS1.
 10. G. -H. Lee, S. Xiao, and A. M. Weiner, "Programmable, polarization-independent, and DWDM-capable chromatic dispersion compensator using virtually-imaged phased-array and spatial light modulator," in *Optical Fiber Communication Conference and Exposition and the National Fiber Optic Engineers Conference*, Technical Digest (CD) (Optical Society of America, 2006), paper OThE5.
 11. L. Grüner-Nielsen, Y. Qian, B. Pálsdóttir, Y. Qian, P. B. Gaarde, S. Dyrbøl, T. Veng, R. Boncek, and R. Lingle, "Module for simultaneous C+L-band dispersion compensation and Raman amplification," in *Optical Fiber Communication Conference*, A. Sawchuk, ed., Vol. 70 of OSA Trends in Optical and Photonics (Optical Society of America, 2002), paper TuJ6.
 12. M. Karásek, P. Peterka, and J. Radil, "Transmission of 2×10 GE channels over 252 km without in-line EDFA," in *Proceedings of Conference on Optical Network Design and Modeling* (IEEE, 2005), pp. 55–58.
 13. M. Karasek, P. Peterka, and J. Radil, "10 gigabit Ethernet long-haul transmission without EDFAs," *Ann. Telecommun.* **61**, 478–488 (2006).
 14. R. J. Nuyts, Y. K. Park, and P. Gallion, "Dispersion equalization of a 10 Gb/s repeatered transmission system using dispersion compensating fibers," *J. Lightwave Technol.* **15**, 31–42 (1997).
 15. M. Karasek, J. Radil, and L. Bohac, "Optimization of NRZ data transmission at 10 Gbit/s over G.652 without in-line EDFAs," *Fiber Integr. Opt.* **23**, 297–310 (2004).